UDC 539.4

Nanomechanical Properties of TiN/TiC Multilayer Coatings

M. Azadi[1] and A. Sabour Rouhaghdam

Tarbiat Modares University, Tehran, Iran

[1] mahbub.azadi@gmail.com

УДК 539.4

Наномеханические свойства многослойных покрытий TiN/TiC

М. Азади, А. Сабур Рухагдам

Тарбиат Модарес университет, Тегеран, Иран

Исследованы структура, состав и механические свойства многослойных покрытий TiN/TiC. Все покрытия наносились на образцы из инструментальной стали марки H13 методом вакуум-плазменного химического осаждения паров с пульсирующим разрядом постоянного тока. С помощью атомно-силового микроскопа были выполнены испытания по внедрению наноиндентора и наноцарапанию. В результате определены такие механические характеристики: твердость, модуль упругости, шероховатость поверхности и коэффициент трения. Для изучения кристаллической структуры покрытий использовались метод скользящей рентгеновской дифракции и туннельная сканирующая микроскопия. Показано, что с увеличением количества слоев покрытий повышаются модуль упругости и твердость. Установлено, что десятислойные покрытия имеют высокие механические характеристики (твердость, модуль упругости, сопротивление царапанию), поэтому покрытия такого типа рекомендуются для использования в случаях, если требуется их повышенная износостойкость.

Ключевые слова: TiN/TiC покрытия, вакуум-плазменное химическое осаждение паров, атомно-силовой микроскоп, наноиндентирование, наноцарапание.

Introduction. Hard coatings such as titanium carbide (TiC) and titanium nitride (TiN) are widely used in various industries. This is due to their unique properties such as high hardness and elastic modulus, satisfactory corrosion and wear resistance, good electrical and thermal conductivities, a well as high melting temperature [1–3]. Since single-layer coatings due to their specific characteristics exhibit less efficient performance than multilayer ones, in recent papers various multilayer coatings were investigated, which have a number of advantages over single-layer coatings. They combine attractive properties of several materials, as well as exhibit some completely new properties that are not observed in single-layer coatings. Each layer in a multilayer coating contributes to the surface with its specific properties. Multilayer coatings have been found to possess better mechanical properties than single-layer ones: for example, higher hardness, fracture toughness and strength [4, 5].

Thin coatings can be deposited by different methods, such as physical vapor and thermal chemical vapor techniques. During implementation of the first method , the coating adhesion strength decreases due to low temperature, whereas the second method implies a high temperature, due to which grain growth occurs and quality of coatings' properties is deteriorated [6, 7]. On the other hand, the pulsed-DC plasma-assisted chemical vapor deposition (PACVD) is a proper technique for depositing thin coatings over different substrates, due to the possibility of achieving the same properties at lower temperatures. Control of composition and thickness of coatings is performed by adjusting plasma

parameters. Moreover, rotation of the complex specimen is no more required [6, 8–9]. It is noteworthy that researchers have been studied TiN/TiC multilayer coatings obtained by other techniques [7, 10], but only few studies were dedicated to the PACVD technique. In addition, due to brittleness of TiC layer, most researchers studied TiN/Ti(C,N)/TiC coatings [7]. Thus, there are only scarce research results on TiN/TiC multilayer coatings. However, such properties as hardness of TiN/TiC double-layer coatings obtained using the PACVD were investigated by Kim et al. [6]. Takahashi et al. [11] also prepared the compositionally graded TiC/TiN films by the liquid injection PACVD and studied the composition and structure of graded TiC/TiN films deposited over silicon substrates.

The objective of this study was to deposit TiN/TiC multilayer coatings over H13 hot work tool steel by the PACVD technique and then to evaluate the influence of the number of layers on nanoindentation characteristics and the scratch resistance of TiN/TiC multilayer coatings. The crystalline structure of coatings is determined by the grazing incidence X-ray diffraction (GIXRD) and the field emission scanning electron microscopy (FE-SEM). The surface morphology, roughness and nanomechanical properties, such as the elastic modulus, hardness, wear and scratch resistance are determined by the atomic force microscopy (AFM) with NanoScope and Hysitron TriboScope instruments.

1. **Material and Methods**. H13 hot work tool steel specimens with the composition listed in Table 1 were heat-treated, in order to increase their hardness. Specimens were prepared by grinding up to surface roughness of 2000 and cleaned with alkali solution in ultrasonic bath at 100℃ for 10 min. In order to increase the adhesion of coatings to the substrate and to increase the load capacity of coatings, a plasma nitriding operation with parameters listed in Table 2 was performed. In the plasma nitriding process, the flow ratio of hydrogen to nitrogen was fixed about 3 to prevent the white layer formation [12].

T a b l e 1

Chemical Composition of the Substrate (wt.%)

C	Si	Cr	Mo	V	Mn	Ni	Cu	Fe
0.45	0.69	5.72	1.14	2.23	0.27	0.15	0.24	balance

T a b l e 2

Parameters Used in the Plasma Nitriding Process

Temperature (°C)	Pressure (mbar)	Duty cycle (%)	Voltage (V)	Time (min)	Hydrogen (sccm)	Nitrogen (sccm)	Argon (sccm)
470	2	33	650	60	1600	500	500

TiN/TiC multilayer and single-layer coatings were deposited in a PACVD reactor, using a $TiCl_4$–Ar–CH_4–H_2–N_2 gas mixture. The plasma was triggered by a pulsed-DC power supply. The total pressure in the reaction chamber was 2–6 mbar. Fixed flow rates of argon, hydrogen and titanium chloride, methane and nitrogen were 500, 1600, 50, 1200, and 250 sccm, respectively. The duty cycle for all specimens was 33%. A negative bias voltage was fixed at 600–650 V during the process in the chamber with height and diameter of 70×50 cm. The substrate temperature was controlled by an auxiliary heating system, in addition to the intrinsic sputtering effect. Other experimental conditions are listed in Table 3. The TiN layer was deposited firstly, in order to have a better adhesion to the substrate [7]. The thickness of each (TiN/TiC) layer in multilayer coatings was controlled by adjusting the feeding time of reactant gases, based on the reference of the deposition rate in TiN/TiC single-layer coatings. The thickness of layers varied from 0.2 to 2 μm.

T a b l e 3

Parameters Used in the Coating Deposition Process

Time (min)	Temperature (°C)	Titanium chloride (sccm)	Methane (sccm)	Nitrogen (sccm)
80	450–470	50	80	250

In this paper, the GIXRD with test specifications of $\alpha = 2°$ (the incidence angle) and the radiation of 1.5418 Å: CuKα was used. For coatings, the cross section was observed by the FE-SEM.

The surface morphology and roughness of coatings were measured by the AFM. Nanomechanical properties such as the elastic modulus (E) and hardness (H) were determined by the nanoindentation (the Hysitron TriboScope instrument). The nanomechanical test instrument with the two-dimensional transducer, complete software and the Berkovich diamond indenter was used after calibrating instruments including the compliance. The indentation time was 10 s. The sensor of the transducer recorded values for the normal force and the normal depth. Five indentation tests for each specimen were conducted in this study. In the AFM part, the NanoScope instrument was also used. Recently, emerging technologies such as the AFM and the surface force apparatus have opened the possibility to study friction and wear phenomena in a molecular scale. This allows one to measure frictional forces between contacting molecules at the nanonewton level [13]. The nanoscratch test has extended the applicability range of the nanoindentation device. The scratch was made by moving the indenter laterally with continuous penetration into the specimen. Every scratch had 4 μm length, and it took 30 s to conduct a scratch test. The friction coefficient of coatings was measured through the nanoscratch test. The normal load of the scratch test was ramped from zero to 2000 μN. The normal force, the lateral force, the normal displacement, and the lateral displacement during the scratch test were recorded with respect to the time. Three scratch tests for each specimen were also conducted in this study.

2. **Results and Discussion**.

2.1. ***X-Ray Diffraction***. Phases of deposited films were identified by the GIXRD. Figure 1 demonstrates the GIXRD pattern obtained from TiN/TiC multilayer and single-layer coatings. These diffraction patterns show the orientation in the direction of crystalline planes including (1 1 1), (2 0 0), (2 2 0), (3 1 1), and (2 2 2) planes. The literature reported that these peaks corresponded to TiN and TiC layers [14]. In multilayer coatings, the peak width and the intensity were more than the peak for TiC or TiN single-layer coatings. Due to the near position of the peak characteristic of the TiC phase or the TiN phase, the peak separation for each layer was not observed in multilayer coatings. This result (overlaying of peaks for each layer in multilayer coatings) was consistent with the result of other researches [15, 16]. The study of the crystal structure of deposited layer coatings showed a texture in the (2 0 0) orientation for all specimens. Therefore, the (2 0 0) plane which had the lowest surface energy was the preferred structure, although the (1 1 1) texture was the common structure of these 4 coatings [17]. In multilayer coatings, depositing of the first layer (the TiN layer) had no effect on the preferred orientation of the grain growth in the second layer (the TiC layer). However, increasing the number of layers (from 2 to 10) caused the increasing tendency in the (1 1 1) texture.

2.2. ***Microstructure of Coatings***. The cross section of single-layer and multilayer coatings was observed by the FE-SEM, as shown in Fig. 2. The total thickness of TiN/TiC multilayer coatings was 2–3 μm, approximately. Investigation of the morphology of all coatings demonstrated a fine-grained structure, whereas coatings which were deposited by the physical vapor deposition [18] had a columnar structure. Layers are closely integrated,

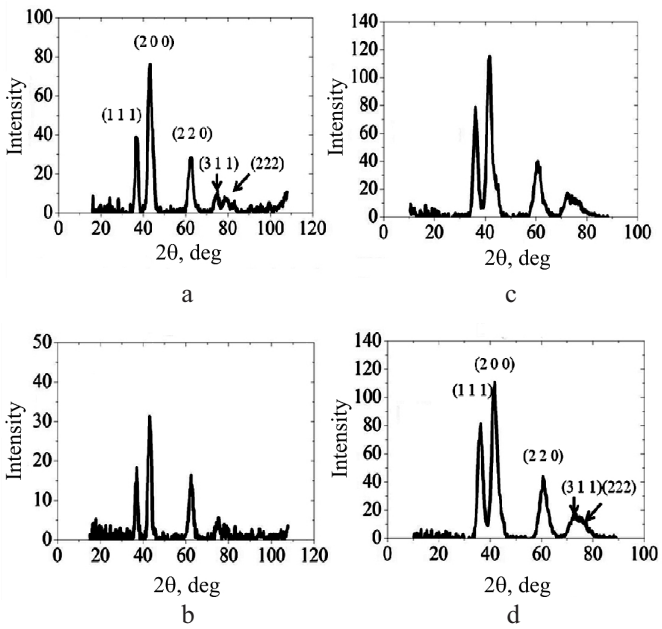

Fig. 1. GIXRD test results for specimens including TiN (a), TiC (b), and multilayer coatings with 2 (c) and 10 (d) layers.

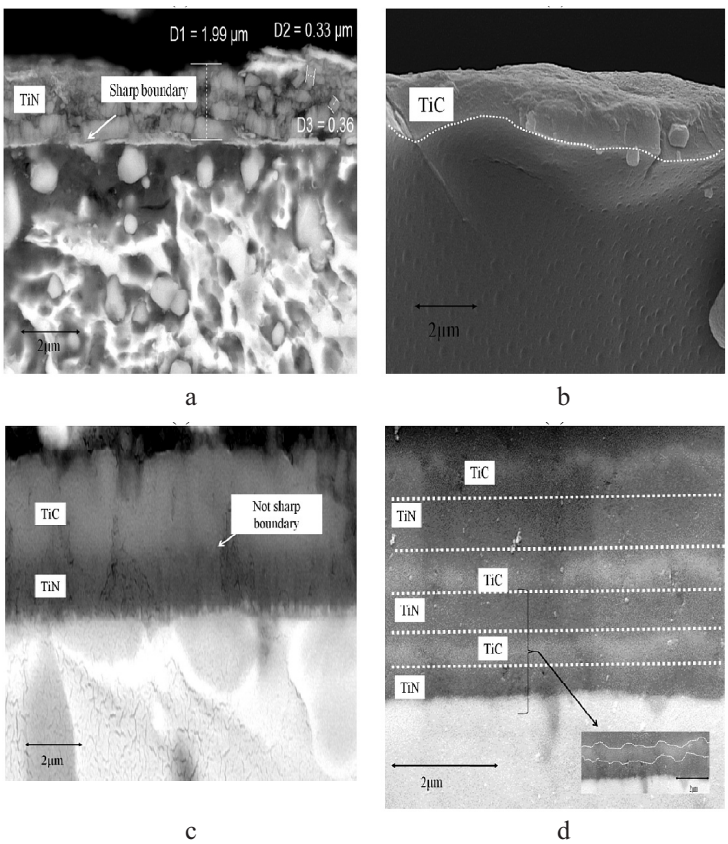

Fig. 2. Cross section FE-SEM images for specimens including TiN (a), TiC (b), and multilayer coatings with 2 (c) and 6 (d) layers.

and the interface between the film and the substrate is flat without pores and defects. This indicates good interfacial bonding properties. By increasing the number of layers, the coating possessed smaller grain structure and the structure became increasingly densed, as reported by Liu et al. [19]. Thus, few spaces and defects have appeared in the coatings. The existence of the multilayer interface structure can reduce the internal stress of the film. As is shown in Fig. 2b, images demonstrate that if the substrate surface is not completely flat, coatings are deposited even in down hills of the surface, and a uniform coating is formed. This is due to the high power throwing property, which is intrinsic only to the PACVD process. The interface between TiN layers and TiC layers in multilayer coatings is not quite sharp (Fig. 2c and 2d).

2.3. ***Surface Morphology***. The AFM was carried out to quantitatively study the surface morphology of specimens in relation with an increase of the number of layers in TiN/TiC multilayer coatings. Figure 3 shows AFM images for coatings that were analyzed in 2×2 μm. Lighter areas of AFM images represent those regions with a higher height. Figure 3 demonstrates that asperities were distributed over a broader range of heights on multilayer coatings, compared to single-layer coatings. This is also confirmed by the roughness and values of the root mean square roughness profile of the surface height (R_{rms}). The grain height in TiN single-layer coating attains the smallest value and is about 65 nm. Some sub-grains in TiN single-layer coating were also observed. As the number of layers in TiN/TiC multilayer coatings was changed from 2 to 10, the grains' height increased from 81 nm to 89 nm. Thus, about the 25–36% enhancement is observed for multilayer coatings, in comparison to the grain height of TiN single-layer coatings. The morphology of grains in TiN single-layer coatings is similar to pyramidal or granular structures, while the grains' shape in other coatings is spherical.

Figure 4 shows the relation between roughness and grain height versus the number of layers, where R_a is defined as the mean value of the surface height relative to the center plane, while R_{rms} is the root mean square roughness profile of the surface height within the scanned area [8]. The results obtained indicate that R_a and R_{rms} are affected by the structure and the material. TiC single-layer coatings exhibit lower surface roughness than other coatings. Increase in the number of layers from 2 to 10 in TiN/TiC multilayer coatings results in the increase of the surface roughness. Variation of the surface roughness with the number of layers exhibits a trend similar to the grain height variation, as is shown in Fig. 4. When the number of layers in TiN/TiC multilayer coatings was increased from 2 to 10, the surface roughness (R_a) also increased from 20 to 26 nm. This corresponds to about 11–44% increase, as compared to the surface roughness of TiC single-layer coatings. It is noteworthy that the surface roughness of coatings is directly related to the surface preparation of the substrate. If the level of the preparation is higher, the coating surface roughness is decreased. In other words, in case of a single-layer coating, when the layer is directly deposited onto the mirror surface of the substrate, the surface roughness attains the minimum value. Therefore, multilayer coatings with 10 layers have the maximum surface roughness among other coatings. As established by Morant et al. [20], there is a relation between increasing the surface roughness and increasing the number of layers in multilayer coatings.

2.4. ***Nanoindentation***. Nanoindentation experiments were performed to study mechanical characteristics as a function of the multilayer wavelength. The dependences between nanohardness, elastic modulus and the number of layers in multilayer coatings are shown in Fig. 5.

The thickness of coatings exceeds the total indentation depth by more than ten times. Hence, hardness and elastic modulus were calculated only for coatings (with no consideration of the substrate effect). For better comparison, hardness values of TiN and TiC single-layer coatings were also reported. Mechanical properties such as hardness (H) and the elastic modulus (E) were calculated by fitting the unloading part of the $P - h$ curve via the Oliver–Pharr method [21–23].

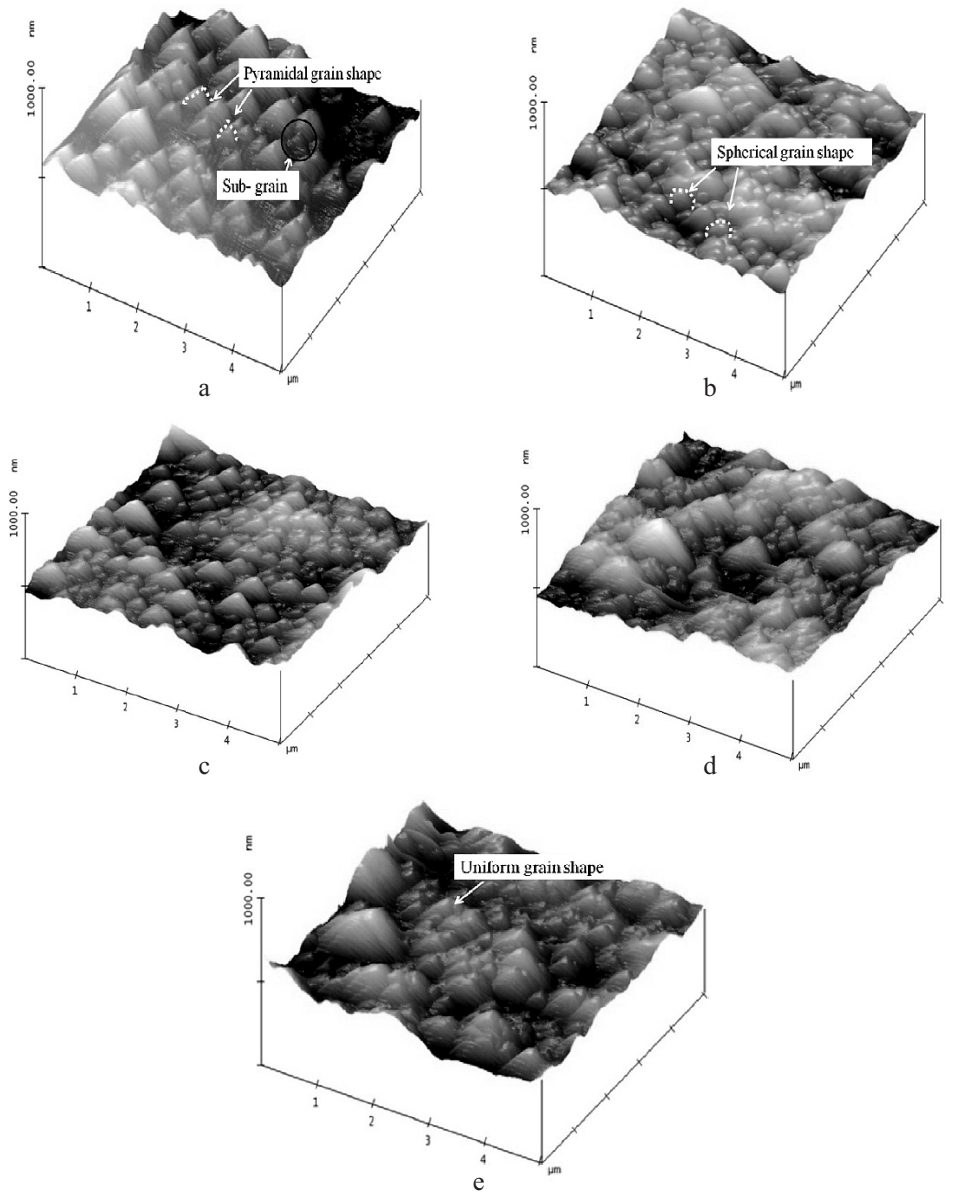

Fig. 3. The three-dimensional AFM image of the surface topography including TiN (a), TiC (b), multilayer coatings with 2 (c), 6 (d), and 10 (e) layers.

Via this method, the contact hardness (H_c) can be obtained from Eq. (1):

$$H_c = \frac{P_{\max}}{A_c} = \frac{P_{\max}}{\alpha h_{\max}^2}, \tag{1}$$

where α is a non-dimensional geometrical constant, $\alpha = \pi \tan^2 \omega c$, in which ω is the inner angle of the effective cone, approximating the pyramidal indenter tip geometry. The value of 24.5 for α is associated with the ideal Vickers or Berkovich pyramidal indenter, with ω of 70.38 [8]. Thus, the hardness is related to the maximum displacement ($h_{\max}$) in

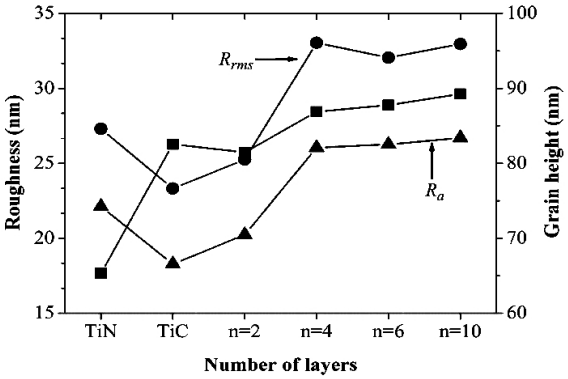

Fig. 4. Relation between roughness (R_a and R_{rms}), grain height, and the number of layers.

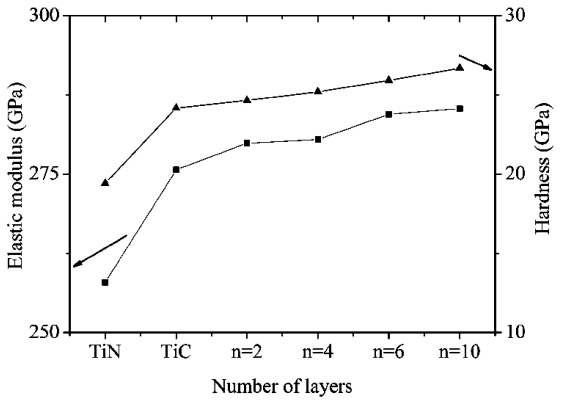

Fig. 5. Relation between nanohardness, elastic modulus, and the number of layers.

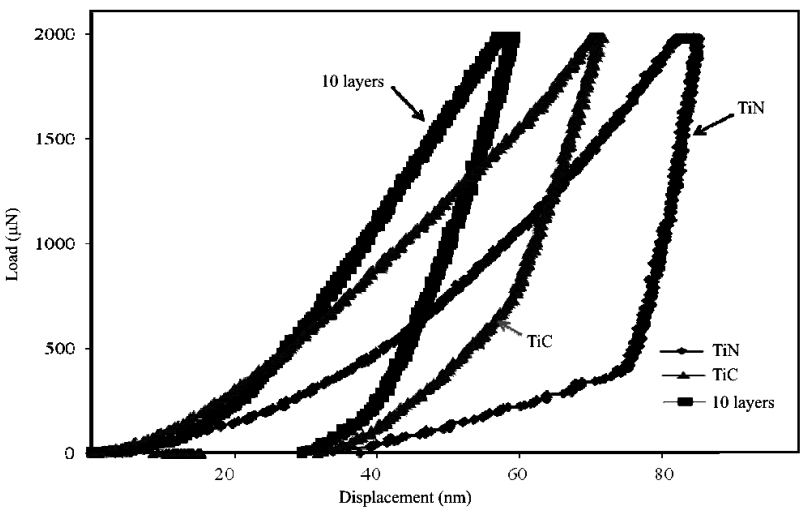

Fig. 6. The loading–unloading curve of specimens including TiC, TiN, and multilayer coatings with 10 layers.

the load–displacement curve. As TiN single-layer coatings have the maximum displacement (Fig. 6), they exhibit lower hardness than other coatings.

All hardness values of multilayer coatings are about 24.6–26.7 GPa, while hardness of TiN and TiC single-layer coatings are about 19.4–24.4 GPa, respectively. The first value (19.4 GPa) was also established by Kim et al. [24]. Moreover, hardness of all multilayer coatings exceeds that of TiC and TiN single-layer ones. As the number of layers is increased, an enhancement can be observed. The hardness of multilayer coatings has reached its maximum value of 26.7 GPa in case of 10 layers. While hardness is related to composition and structure of single-layer coatings, high hardness values can be also atrributed to the role of interfaces as effective obstacles for the lattice dislocation slip and the dominant deformation mechanism in multilayer coatings [5, 17]. The maximum hardness by interface strengthening can be described by the following simple equation. Consider a multilayer structure containing two layers, one of which (layer A) has a low shear modulus, while the other (layer B) has a high shear modulus. Therefore,

$$H_{\max} = H_A + \frac{3(G_B - G_A)\sin\theta}{m\pi^2}, \tag{2}$$

$$G = \frac{E}{2(1+\nu)}, \tag{3}$$

where H_A is hardness of layer A (with a lower shear modulus), G is shear modulus, θ is angle between the interface and the slip plane of layers, and m is the Taylor factor. The value of m can be estimated as 0.3 for transition metal nitrides in NaCl type structures. Poisson's ratio (ν) is 0.24–0.25 for TiC and TiN coatings. Hardness and elastic modulus values of individual layers are obtained through nanoindentation tests [21]. Thus,

$$H_{\max} = H_A + 0.1044(E_B - E_A). \tag{4}$$

Results for TiN/TiC multilayer coatings show a difference between experimental data of nanoindentation tests and results derived from interface characteristics through Eq. (4). We have found that this difference is caused by dislocation blocking in the system of multilayer coatings. Therefore, the highest hardness was found for multilayer coatings with 10 layers, reaching the maximum value of 26.7 GPa. Thus, the increase in hardness is equal to 38% , which is higher the expected referent value (34%) from the rule-of-mixtures applied to TiC and TiN coatings. Explanation for this hardness enhancement in TiN/TiC multilayer coatings can be based on interfaces acting on dislocations and Hall–Petch models, which provide a good overall picture of hardness enhancements [25].

The PACVD is a technique which allows one to generate compressive stresses in the most coatings [26]. In addition, as established by Ding et al. [27], increase in the number of layers in multilayer coatings results in augmentation of the compressive stress and hardness values [28]. Thus, hardness of TiN/TiC multilayer coatings was also increased due to generation of the compressive stresses. Enhanced hardness values have been also observed in the process of material bombardment by high-energy ions during deposition of coatings with high compressive stresses in [8].

The stiffness ($S = dP/dh$) of the contact can be used to calculate the reduced elastic modulus (E_r) via the following equation:

$$E_r = \frac{1}{\beta}\frac{\sqrt{\pi}}{2}\frac{S}{\sqrt{A_p(h_c)}}, \tag{5}$$

where $A_p(h_c)$ is the projected area of the indentation at the contact depth (h_c) and β is a geometrical constant $A_p(h_c)$ is often approximated by a fitting polynomial for the

Berkovich tip [29]. The area function of this indenter is calibrated by the B270 glass. The variation of E with the number of layers exhibited a trend similar to that of the variation of H, as shown in Fig. 5. During the increase in the number of layers, the elastic modulus was reported to increase linearly.

The wear resistance can be predicted by the elasticity index (H/E), describing the elastic strain prior to failure. This ratio is the measure of the ability to absorb the energy elastically. In addition, H^2/E defines the resistance to fracture (the Irwin–Orowan–Griffith case). Tough materials are characterized by high H^2/E [30]. High H/E and H^2/E values are intrinsic to multilayer coatings, in contrast to single-layer ones, as it is shown in Table 4. Although for a long time the hardness has been regarded as a primary material property affecting the wear resistance, the elastic strain prior to failure seems to be a suitable parameter for predicting the wear resistance [9, 22, 31]. Thus, with increase in the number of layers from 2 to 10 in TiN/TiC multilayer coatings, the wear resistance or the H/E ratio is also increased (by about 7%, in comparison to TiC single-layer coatings), while the fracture toughness or the H^2/E ratio is also increased (by about 17%, in comparison to TiC single-layer coatings).

T a b l e 4

Nanomechanical Properties Obtained by the AFM

Coatings type	Number of layers	H/E	H^2/E	μ	Lateral force (μN)	Normal displacement (nm)
TiN	$n=1$	0.0713	1.46	0.28	673±10	157±2
TiC	$n=1$	0.0876	2.12	0.33	727±10	86±2
2 layers	$n=2$	0.0880	1.85	0.30	690±10	134±2
4 layers	$n=4$	0.0898	2.26	0.31	681±10	112±2
6 layers	$n=6$	0.0910	2.36	0.33	685±10	105±2
10 layers	$n=10$	0.0935	2.49	0.34	734±10	88±2

2.5. ***Nanoscratch***. The AFM has been shown to be a powerful tool to investigate the nanofriction behavior of several surfaces, including metals, ceramics and polymers [32]. Friction coefficients (ratio of the measured friction force to the applied normal force) for all coatings were calculated as an average of about 400 data points over the entire sliding distance. Figure 7 shows variation of friction coefficients with the scratch time. Based on the nanoscratch data, changes in the relative elastic-plastic response can be monitored. During the running-in time, due to the interaction between the tip and asperities on coatings, the friction coefficient (μ) is increased. At the initial stage, the friction coefficient is controlled by the film roughness and the build-up of a transfer layer (tribolayer). At the second stage, friction and wear are controlled by the nature of the tribolayer [33]. The average value of friction coefficients (μ) for all multilayer coatings was approximately 0.3–0.34. The minimum average value of friction coefficients (0.28) was related to TiN single-layer coatings. Thus, when the number of layers was increased, the increase in the friction coefficient was also observed. This result shows that multilayer coatings have better scratch resistance, as compared to TiN single-layer ones. This suggests a dependency between the surface asperity, roughness, hardness, and the friction coefficient by this scale for TiN/TiC multilayer coatings. This occurrs when the loading rate, scratching speed, indenter tip radius and the indenter material remain unchanged during the scratch test.

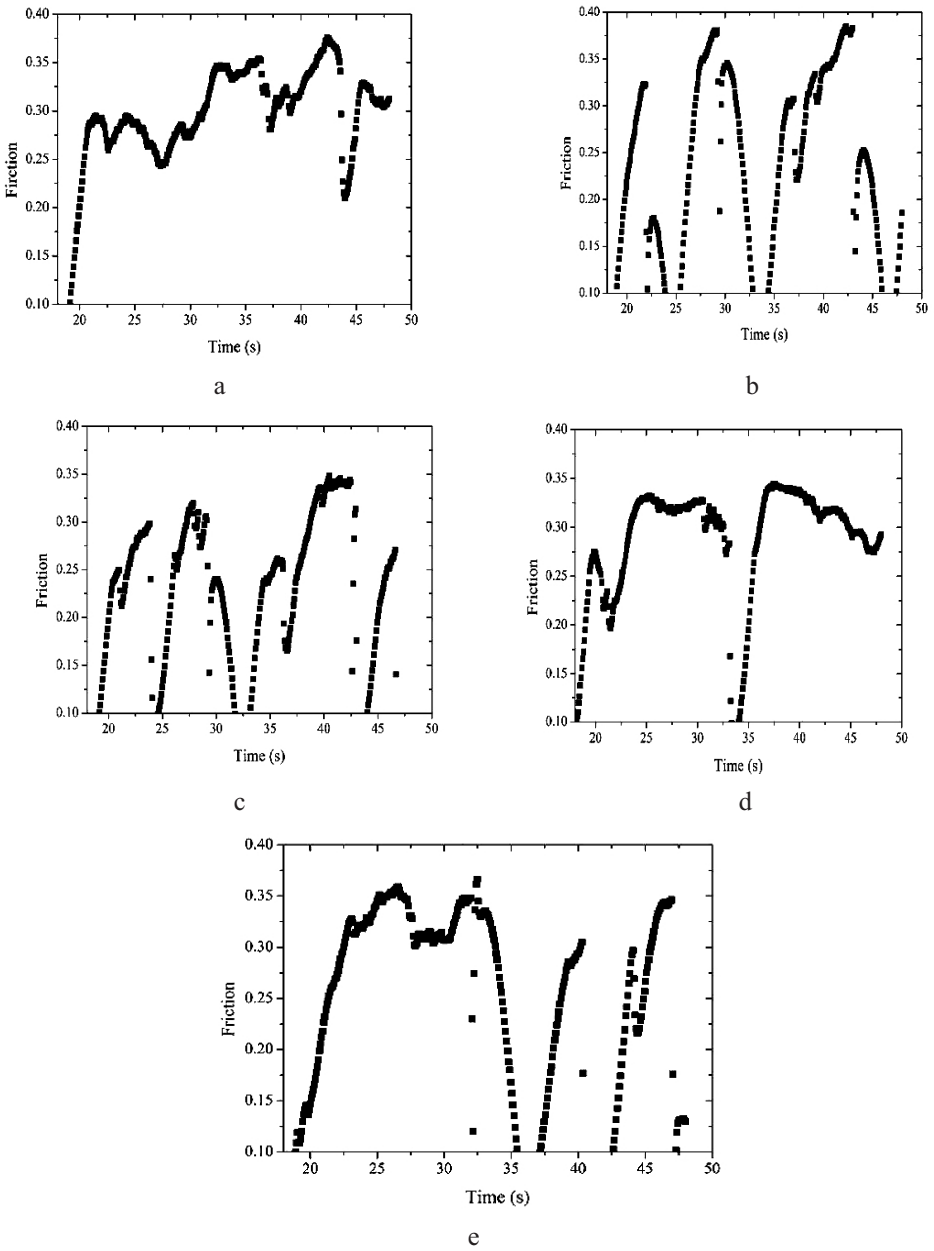

Fig. 7. Friction coefficient versus time for different specimens including TiN (a), TiC (b), multilayer coatings with 2 (c), 6 (d), 10 (e) layers.

According to Recco et al. [34], when the coating hardness is increased, the friction coefficient is also increased. Variation of the friction coefficient in TiN single-layer coatings with the scratch time was approximately fixed and the diagram was continuous over the scratch time, but similar diagrams for other coatings were discontinuous, whereas this discontinuity exhibited a certain improvement in the scratch resistance. When the number of layers in multilayer coatings is increased, variation of friction coefficients is slowly increased over the scratch time. According to the lateral (shear) force shown in Table 4, the critical load for multilayer coatings with 10 layers is higher than that in other

coatings, whereas the critical loads for other multilayer coatings are lower than in TiC single-layer coatings. The normal displacement that describes the scratch depth turned ot to be similar in multilayer coatings with 10 layers and TiC single-layer ones. This indicates that the scratch resistance of multilayer coatings, especially those with 10 layers, is higher than that of TiN single-layer coatings.

Conclusions. TiN/TiC multilayer coatings were successfully deposited by the pulsed-DC PACVD with the number of layers ranging from 2 to 10. High hardness values (about 26.7 GPa) are observed for TiN/TiC multilayer coatings deposited with 10 layers. The enhanced hardness of multilayer coatings is attributed to several interfaces which block the dislocation motion across the interface between Ti–C and Ti–N layers. This is due to differences in the shear moduli of materials in the individual layers. The values of hardness and elastic modulus of TiN/TiC multilayer coatings are found to be slightly higher than those observed in single-layer coatings. The results obtained show that the TiN film has the smallest grain height, whereas the TiC film has the lowest surface roughness. By increasing the number of layers from 2 to 10 in multilayer coatings, it became possible to increase the grain height, surface roughness, hardness, elastic modulus, as well as wear and scratch resistance of the coatings.

Р е з ю м е

Досліджено структуру, склад і механічні властивості багатошарових покриттів TiN/TiC. Всі покриття наносилисй на зразки з інструментальної сталі марки Н13 методом вакуум-плазмового хімічного осадження парів із пульсуючим розрядом постійного струму. За допомогою атомно-силового мікроскопа було проведено випробування на проникнення наноіндентора та наноцарапання. У результаті визначено такі механічні характеристики: твердість, модуль пружності, шорсткість поверхні і коефіцієнт тертя. Для вивчення кристалічної структури покриттів використовувались метод ковзної рентгенівської дифракції і тунельна сканувальна мікроскопія. Показано, що збільшення кількості шарів покриттів приводить до росту модуля пружності і твердості. Установлено, що покриття з десяти шарів мають високі механічні характеристики (твердість, модуль пружності, опір царапанню), тому покриття такого типу рекомендуються для використання у випадку, якщо потребується їх підвищена зносостійкість.

1. H. Liepack, K. Bartsch, W. Brückner, A. Leonhardt, “Mechanical behavior of PACVD TiC–amorphous carbon composite layers,” *Surf. Coat. Technol.*, **183**, 69–73 (2004).
2. N. Kumar, R. Krishnan, D. Dinesh Kumar, et al., “Tribological properties of nanostructured TiC coatings deposited on steel and silicon substrates using pulse laser deposition technique,” *Tribology – Mater. Surf. Interfaces*, **5**, 1–9 (2011).
3. A. Shanaghi, A. Sabour Rouhaghdam, S. Ahangarani, et al., “Effects of duty cycle on microstructure and corrosion behavior of TiC coatings prepared by DC pulsed plasma CVD,” *Appl. Surf. Sci.*, **258**, 3051–3057 (2012).
4. P. Panjan, M. Ekada, D. Kek-Merl, et al., “Deposition and characterization of $Ti_{0.5}Al_{0.5}N$/CrN multilayer coating sputtered at low temperature,” *MTAEC9*, **37** (3-4), 123–127 (2003).
5. J. Lim, J. Lee, H. Ahn, and K. T. Rie, “Mechanical properties of TiNyTiB2 multilayers deposited by plasma enhanced chemical vapor deposition,” *Surf. Coat. Technol.*, **174-175**, 720–724 (2003).
6. D. Kim, Y. Cho, M. Lee, et al, “Properties of TiN–TiC coatings using plasma-assisted chemical vapor deposition,” *Surf. Coat. Technol*., **116-119**, 906–910 (1999).

7. Y. Zhao, G. Lin, J. Xiao, et al., "TiN/TiC multilayer films deposited by pulse biased arc ion plating," *Vacuum*, **85**, 14 (2010).
8. A. Shanaghi, A. Sabour Rouhaghdam, S. Ahangarani, and P. K. Chu, "Effect of plasma CVD operating temperature on nanomechanical properties of TiC nano-structured coating investigated by atomic force microscopy," *Mater. Res. Bull*., **47**, 2200–2205 (2012).
9. H. L. Wang, J. L. He, and M. H. Hon, "Sliding wear resistance of TiCN coatings on tool steel made by plasma-enhanced chemical vapor deposition," *Wear*, **169**, 195–200 (1993).
10. Y. Iwai, T. Miyajima, A. Mizuno, et al., "Micro-slurry-jet erosion (MSE) testing of CVD TiC/TiN and TiC coatings," *Wear*, **267**, 264–269 (2009).
11. M. Takahashi and S. Shimada, "Preparation of composite and compositionally graded TiC–TiN films by liquid injection plasma-enhanced CVD," *Solid State Ionics*, **172**, 249–252 (2004).
12. S. Ma, Y. Li, and K. Xu, "The composite of nitrided steel of H13 and TiN coatings by plasma duplex treatment and the effect of pre-nitriding," *Surf. Coat. Technol.*, **137**, 116–121 (2001).
13. K. Holmberg, A. Matthews, and H. Ronkainen, "Coatings tribology-contact mechanisms and surface design," *Tribol. Int.*, **31**, 107–120 (1998).
14. A. Devia, V. Benavides, E. Restrepo, et al., "Influence substrate temperature on structural properties of TiN/TiC bilayers produced by pulsed arc techniques," *Vacuum*, **81**, 378–384 (2006).
15. D. E. Wolfe, J. Singh, and K. Narasimhan, "Synthesis and characterization of multilayered TiC–TiB2 coatings deposited by ion beam assisted, electron beam physical vapor deposition (EB-PVD)," *Surf. Coat. Technol.*, **165**, 8–25 (2003).
16. K. T. Rie, A. Gebauer, J. Wohle, et al., "Synthesis of TiN/TiCN/TiC layer systems on steel and cermet substrates by PACVD," *Surf. Coat. Technol.*, **74-75**, 375–381 (1995).
17. C. Jarms, H. R. Stock, H. Berndt, et al., "Influence of the PACVD process parameters on the properties of titanium carbide thin films," *Surf. Coat.Technol.*, **98**, 1547–1552 (1998).
18. Y. T. Pei, D. Galvan, J. Th. M. De Hosson, and C. Strondl, "Advanced TiC/a-C:H nanocomposite coatings deposited by magnetron sputtering," *J. Europ. Ceram. Soc.*, **26**, 565–570 (2006).
19. C. Liu, K. Liu, H. Yan, et al., "Mechanical properties of TiN/NbN multilayered films prepared by PVD coating," *Adv. Ceram. Sci. Eng. (ACSE)*, **2**, 16–22 (2013).
20. C. Morant, P. Prieto, A. Forn, et al., "Hardness enchancement by CN–TiCN–TiN multilayer films," *Surf. Coat. Technol.*, **180-181**, 512–518 (2004).
21. S. H. Kim, Y. J. Baik, and D. Kwon, "Analysis of interfacial strengthening from composite hardness of TiN/VN and TiN/NbN multilayer hard coatings," *Surf. Coat. Technol*., **187**, 47–53 (2004).
22. K. H. T. Raman, M. S. R. N. Kiran, U. Ramamurty, and G. Mohan Rao, "Structure and mechanical properties of Ti–C films deposited using combination of pulsed DC and normal DC magnetron co-sputtering," *Appl. Surf. Sci.*, **258**, 8629–8635 (2012).
23. W. C. Oliver and G. M. Phar, "An improved technique for determining hardness and elastic modulus using load and displacement sensing indentation experiments," *J. Mater. Res.*, **7**, 1564–1583 (1992).

24. S. H. Kim, H. Park, K. H. Lee, et al., "Structure and mechanical properties of titanium nitride thin films grown by reactive pulsed laser deposition," *Process. Res.*, **10**, 49–53 (2009).

25. J. C. Caicedo, C. Amaya, L. Yate, et al., "TiCN/TiN/CN multilayer coatings with enhanced mechanical properties," *Appl. Surf. Sci.*, **256**, 5898–5904 (2010).

26. K. Holmberg, H. Ronkainen, A. Laukkanen, et al., "Residual stresses in TiN, DLC and MoS2 coated surfaces with regard to their tribological fracture behavior," *Wear*, **267**, 2142–2156 (2009).

27. J. Ding, Y. Meng, and S. Wen, "Mechanical properties and fracture toughness of multilayer hard coatings using nanoindentation," *Thin Solid Films*, **371**, 178–182 (2000).

28. A. J. McGinnis, T. R. Watkins, and K. Jagannadham, "Residual stresses in a multilayer system of coatings," *Int. Centre Diffr. Data*, **41**, 443–454 (1999).

29. S. Jian, G. Chen, and T. Lin, "Berkovich nanoindentation on AlN thin films," *Nanoscale Res. Lett.*, **5**, 935–940 (2010).

30. J. M. Lackner, L. Major, and M. Kot, "Microscale interpretation of tribological phenomena in Ti/TiN soft-hard multilayer coatings on soft austenite steel substrates," *Bull. Polish Acad. Sci. (Tech. Sci.)*, **59**, 343–355 (2011).

31. Y. T. Pei, D. Galvan, J. Th. M. De Hosson, and A. Cavaleiro, "Nanostructured TiC/a-C coatings for low friction and wear resistant applications," *Surf. Coat. Technol.*, **198**, 44–50 (2005).

32. L. Ipaz, A. Esguerra-Arce, W. Aperador, et al., "Nanofriction study using atomic force microscopy (AFM) of multilayers based in titanium, chromium and aluminum," in: A. Mendez-Vilas (Ed.), *Current Microscopy Contributions to Advances Science and Technology* (2012), pp. 1395–1403.

33. D. G. Liu, J. P. Tu, C. D. Gu, et al., "Tribological and mechanical behaviors of TiN/CNx multilayer films deposited by magnetron sputtering," *Thin Solid Films*, **519**, 4842–4848 (2011).

34. A. A. C. Recco, C. C. Vifara, A. Sinator, and A. P. Tschiptschin, "Energy dissipation in depthsensing indentation as a characteristic of the nanoscratch behavior of coatings," *Wear*, **267**, 1146–1152 (2009).

Received 19. 09. 2013